Available online at www.eccomasproceedia.org
Eccomas Proceedia COMPDYN (2017) 815-833

ECCOMAS
Proceedia

COMPDYN 2017
6th ECCOMAS Thematic Conference on
Computational Methods in Structural Dynamics and Earthquake Engineering
M. Papadrakakis, M. Fragiadakis (eds.)
Rhodes Island, Greece, 15–17 June 2017

PERFORMANCE ASSESSMENT OF CONCENTRICALLY BRACED FRAMES WITH MODIFIED BRACES DEPENDING ON THE APPLIED BEAM-COLUMN JOINTS

Tzvetan S. Georgiev[1], Dimo S. Zhelev[2], Lora D. Raycheva[3]

[1] Assoc. Prof. Dr. Eng., FCE, University of Architecture, Civil Engineering and Geodesy
1 Hr. Smirnenski blvd., Sofia 1046, Bulgaria
e-mail: cvgeorgiev_fce@uacg.bg

[2] Dr. Eng., Ircon ltd.
2l Samokovsko shose str., Sofia 1138, Bulgaria
e-mail: d.siderov@irconltd.com

[3] Eng., PhD candidate, FCE, University of Architecture, Civil Engineering and Geodesy
1 Hr. Smirnenski blvd., Sofia 1046, Bulgaria
e-mail: raycheva_fce@uacg.bg

Keywords: Improved seismic performance, CBF, Innovative systems, Non-linear analysis, Residual drifts.

Abstract. *Concentrically braced frames with crossed diagonals (X-CBFs) are a popular and traditional system in seismic resistant design. Their energy dissipation capacity is primarily provided by yielding of braces in tension and buckling in compression. An improved CBF configuration by introducing bracings with modified sections, resulting in low cycle fatigue endurance and enhanced ductility of the critical member, has been developed during an experimental and numerical research program. Apart from improved dissipative behaviour, proper structural seismic performance implies control over residual drifts and self-centering features of the seismic resistant systems. In that direction proper collaboration between the braces in CBF and contour frame has to be established and improvement of structural performance might be achieved by the engineer at a very affordable level. The beam-to-column joints and the column bases in the contour frame in CBF's could be designed as rigid, semi-rigid or pinned. The connection behaviour has a major influence on the residual drifts of the system. That effect was investigated in series of braced frames with different types of joints. Numerical simulation by nonlinear time history analysis and a detailed comparison is presented. Recommendations for the joints stiffness in CBF with modified braces and assessment of their seismic performance are presented. Different techniques for modelling of the braces as Multi-linear Plastic Link with Pivot hysteresis type and three-hinge model are compared.*

Peer-review under responsibility of the organizing committee of COMPDYN 2017.
doi: 10.7712/120117.5459.17857

1 INTRODUCTION

Concentrically braced frames (CBFs) are a traditional structural system in steel construction. They are used for resisting lateral forces due to wind, earthquakes and others. This system has proved its efficiency for lateral loads by providing sufficient stiffness and strength due to its complete truss action. That is the main reason for its popularity. Nowadays CBFs are widely implemented in a large variety of steel structures.

Contemporary seismic design requires that the lateral force resisting system should have adequate strength and stiffness, but also ductility and energy dissipation capacity. Requirements should be tuned according to the seismicity of the site and the structural performance level demand. It has been observed from earthquakes in the past that severe concentrations of plastic deformation accumulate in the mid-length sections of some bracing members in CBFs. The result of such structural response would be insufficient ductility and energy dissipation capacity illustrated by premature brace fracture and frame failure. Such non-satisfactory seismic behaviour demands improvement of the design practice.

In search of practical and affordable solution for CBFs design, during the period 2011-2012 in the University of Architecture, Civil Engineering and Geodesy (UACEG) in Sofia, a National Research Project was carried out. It was focused on the improvement of the seismic behaviour of braced frames. During the project concentrically braced frames with modification of the braces (acronym CBF-MB) were designed, tested and elaborated. Enhancement of the structural performance requires improved ductility and adequate energy dissipation from one side and self-centering capability from the other. Following that direction, the research on the effect of frame joint types on the structural seismic performance is a matter of interest.

2 DESCRIPTION OF THE CBF-MB SYSTEM

The CBF-MB system emanates from the traditional X-CBFs and modifies them by supplementing two types of innovations [1], [2]. A classical single storey frame of the proposed system consists of columns, diagonal braces, beam and splitting beam (Figure 1). The columns and beams are non-dissipative elements. The columns may be designed with hot rolled HEA or HEB sections. In order to facilitate frame joints and connections design, it is preferable to orientate the column with its web coinciding with the frame plane. The beams are located at floor level and could be of IPE or HEA cross sections, enabling easy detailing of the frame joints. The diagonals are the main dissipative elements while splitting beams may, in some cases, play a partial role in energy dissipation.

The first type of innovation typical for the system is the introduction in the frame of a horizontal intermediate member called a splitting beam. It aims at separating the diagonals thus making them identical and non-interacting (Figure 1). Except for facilitating the detail of the joint between crossing diagonals, the splitting beam stiffness is of essential importance. Splitting beam in cooperation with columns has a crucial impact on the brace buckling sequence and on the type of global plastic mechanism. That issue was studied and discussed in [3]. Moreover, splitting beams with CBF columns constitute an internal elastic backup system that provides good self-centring capacity of the main lateral force resisting system. In that sense, frame joints are an essential part of the system, influencing the overall structural performance.

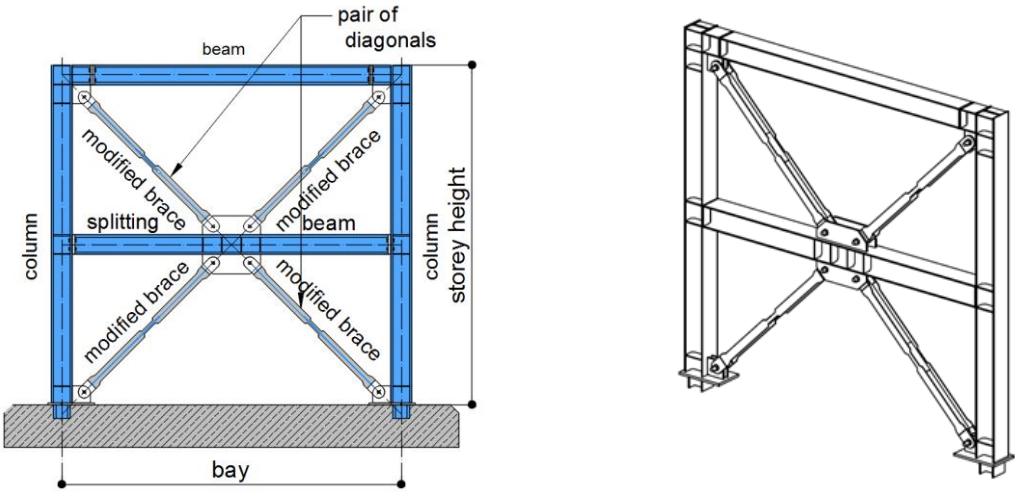

Figure 1: The CBF-MB system

The second type of innovation refers to the introduction of a variable "H"-shaped welded built-up cross-section for the diagonals. Further in the explanation diagonals will be named modified braces (MB). The MB flanges and webs vary along the member length so that zones with different cross-sections are defined as illustrated in Figure 2. The end zones of the diagonals are strengthened by increasing flange widths and thicknesses and are named strong sections (SS). That also allows for an easy connection design and provides fully elastic response of the end zones. In the middle part of the diagonal a modified cross-section (MS) is introduced. It is characterized by reduced bending stiffness and increased cross-sectional area, thus MS is weakened for bending and strengthened for axial forces (Figure 3). The reduced cross section (RS), which is characterized by a lower axial load capacity than MS, is located between the end zone and the middle section.

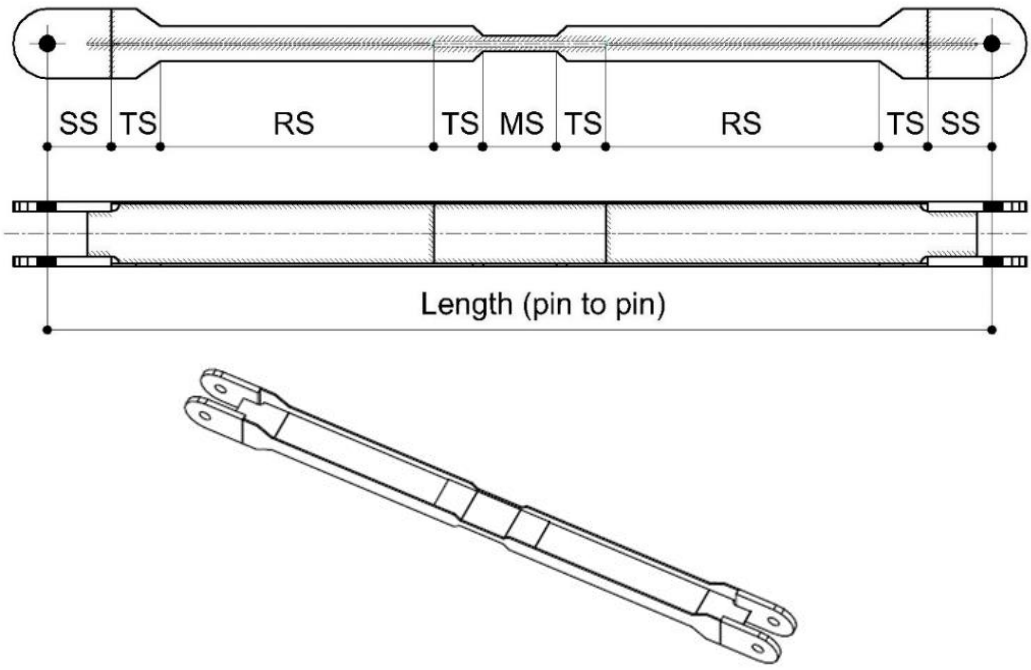

Figure 2: Overview of a modified brace member

Interposed between MS, RS and SS are transition sections (TS). It is the authors' intention that the mode of brace buckling in compression is pre-defined and that full concentration of plastic strains due to bending is achieved in the middle MS. In load reversal, tensile force appears and the element is straightened. Any plastic strains are directed to the reduced cross-section RS rather than to the MS. Thus, the diagonal is designed in a manner that yielding in tension and post-buckling flexural plastic strains occur in different zones along the brace length. That differentiation of the zones with inelastic strains leads to improved low cycle fatigue endurance and avoidance of premature failure of the diagonals. Finally, it reflects in overall improvement of the system hysteretic behaviour and dissipation capacity. The introduction of an "H"-shaped and welded built-up cross-section enables the designer to vary the flange and web thicknesses, heights and widths, and, consequently, to tune the MB design to the particular need of the structure. This makes achieving the controversial code requirements [4] for brace slenderness limitations and homogeneous dissipative behaviour of the diagonals in all storeys much easier.

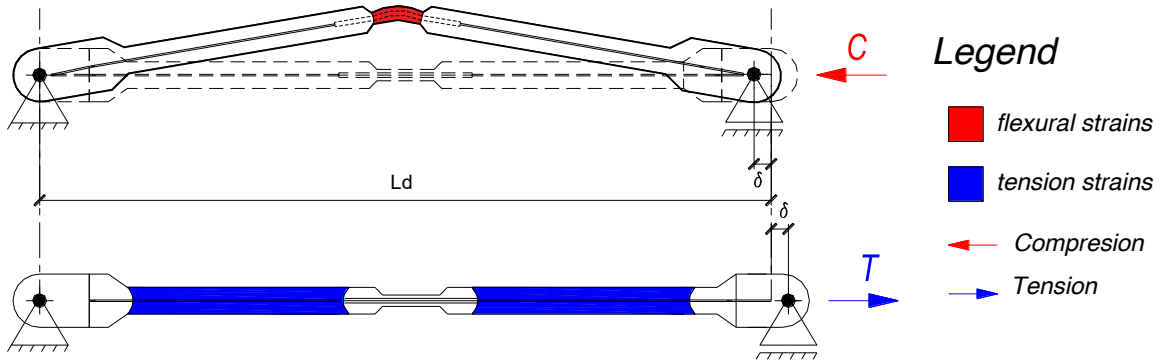

Figure 3: The principle of inelastic cyclic behaviour of MB

Excessive overstrength in steel material for dissipative elements leads to uneconomical design of the non-dissipative elements. In that perspective, a built-up welded cross-section might be composed of S235 steel sheets, unlike hot rolled sections.

3 BRACE MODELING TECHNIQUES

Different modelling techniques can be applied for the numerical simulation of modified brace non-linear behaviour. A single diagonal may be simulated by a concentrated plasticity approach using three hinges. One hinge should be inserted in the middle of the member, simulating flexural plasticity, and two hinges in the quarters, simulating tension yielding. Such a model will be referred to as the 3-Hinge Model (3HM) hereafter. It is important to note that based on calibration with experimental results [5], it was concluded that one brace should be modelled by two FE and that an initial bow imperfection of 1/400 should be applied in the mid node.

Another approach applied herein is simulating the brace non-linear behaviour by single Multi-linear Plastic Link with Pivot hysteresis type [6], [7], named NLL. The non-linear link element used in the SAP2000 model is constituted by several parameters. The pivot points for directing the pivot hysteresis are located by the parameters α_1, α_2, β_1 and β_2. They were calibrated to the experimental results [5] and the resulting values are presented in Table 1.

Pivot point parameter	α_1	α_2	β_1	β_2	η
Value	100	0,1	0,02	0,4	0,0

Table 1: Parameters for directing the pivot hysteresis

3.1 A Single brace under reversal axial displacement

The proposed 3HM and NLL single brace models were compared to a detailed FE model in ANSYS using a calibrated material model of Chaboche [8] and a FE type SHELL181 with mesh size of 10 mm [9]. A cyclic test was conducted by applying incremental fully symmetrical axial displacement and the obtained hysteretic curves are plotted on Figure 4. Typically, a single brace hysteresis exhibits a progressive reduction in compression capacity in subsequent loading cycles. It can be concluded that the hysteretic behaviour of the brace is well captured by the 3HM, and what is more, the resultant curve is very close to the detailed FE model curve in the compression area. The NLL brace hysteretic behaviour deviates more from the detailed FE model curve mainly due to the features of the pivot hysteresis type. It can be noted that when reloading in a positive direction, NLL does not capture the typical pinching and overestimating brace stiffness and strength in the range of small elongations.

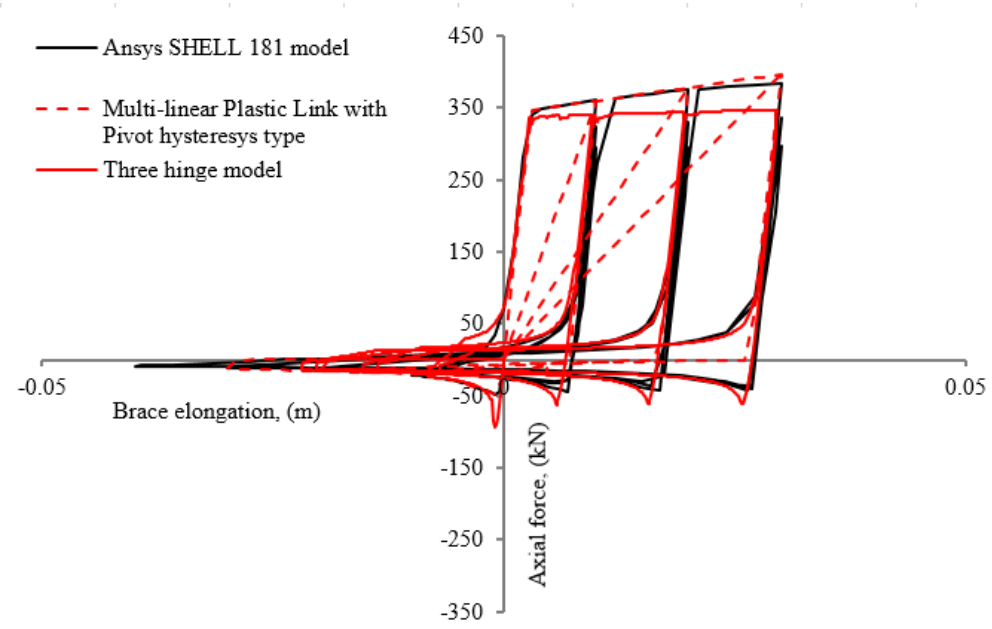

Figure 4: A single MB hysteresis

3.2 Verification of single storey CBF models

The validity of the proposed modelling techniques was confirmed by calibrating numerical to experimental results for a single story CBF-MB. The experimental program involved a displacement-controlled cyclic test of a single story CBF-MB specimen. The adopted loading protocol was consistent with the ECCS recommendations [10]. Details about the experimental programme the reader may find in [1]. The FE models of the test specimen were created following the proposed modelling techniques, namely 3HM and NLL using SAP2000 [7]. For the definition of MB, material with yield strength corresponding to the actual yield strength of the test specimen was used. The material was determined by a standard tensile test in accordance with ISO 6892-1 [11]. The joints between the beams and the columns and column bases

were modelled as semi-rigid, and the joints between the splitting beam and the columns were modelled as pinned, representing the actual test specimen conditions. Figure 5 illustrates the comparison between the hysteresis loops for the test specimen and both FE models (NLL and 3HM). It is indicative that the proposed nonlinear link and three hinge models represent reliably the experimental results. A maximum deviation can be observed in a small displacement region, where the pinching effect in the experimental curve is more severe compared to the computer simulations. It was considered that the computer simulations by 3HM and NNL is reliable and may be used for analytical studies.

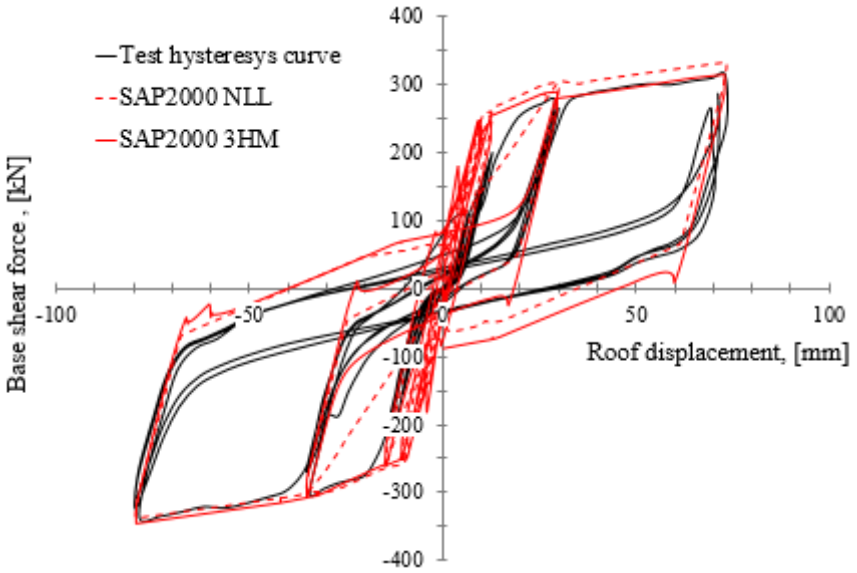

Figure 5: Comparison of hysteresis loops of single story CBF-MB

3.3 Nonlinear dynamic analysis of three story CBF-MB with proposed modelling techniques

The proposed techniques for modelling of modified braces (NLL and 3HM) have also been verified by a nonlinear dynamic analysis of three story CBF-MB FE models under ideal joint conditions: pinned column bases, rigid splitting-beams-to-columns joints and pinned beams to columns. A fibre finite element model developed in SeismoStruct [12] was used as a reference model. The SeismoStruct model had been previously calibrated with experimental hysteresis of a single story CBF-MB. Some useful guidelines for fibre FE modelling may be found in [13]. The three FE models were subjected to a family of ten ground motion records adjusted as to comply with the recommendations of [4].

The base shear force and the roof displacement were used as representative parameters of the models. Their variation in time is illustrated in Figure 6 and Figure 7 for two of the seismic ground motion records (Kobe and Hector Mine). The results from the NLL, 3HM and fibre SeismoStruct models are compared.

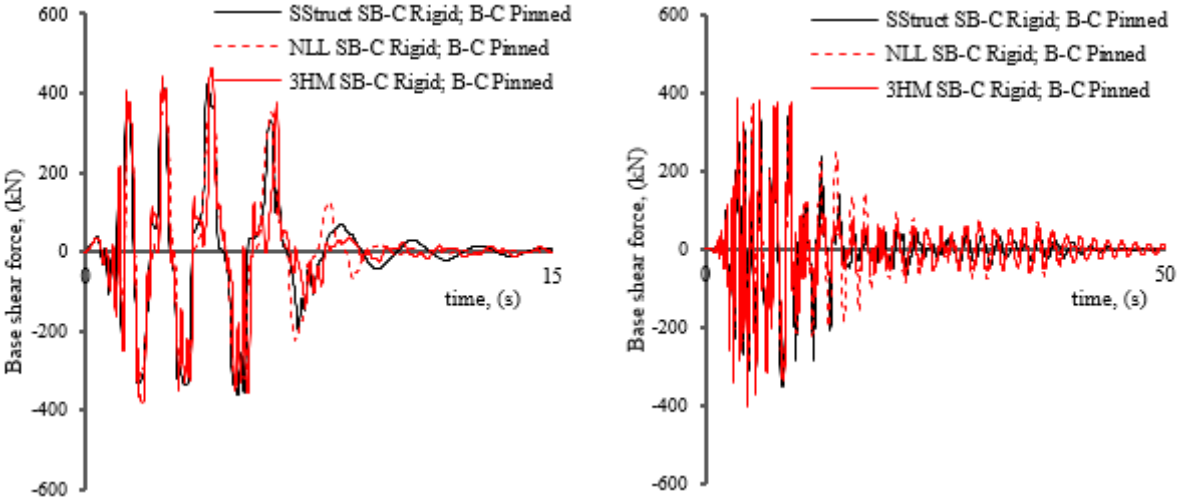

a) Hector mine accelerogram b) Kobe accelerogram

Figure 6: Comparison of 3 story CBF-MB base shear force

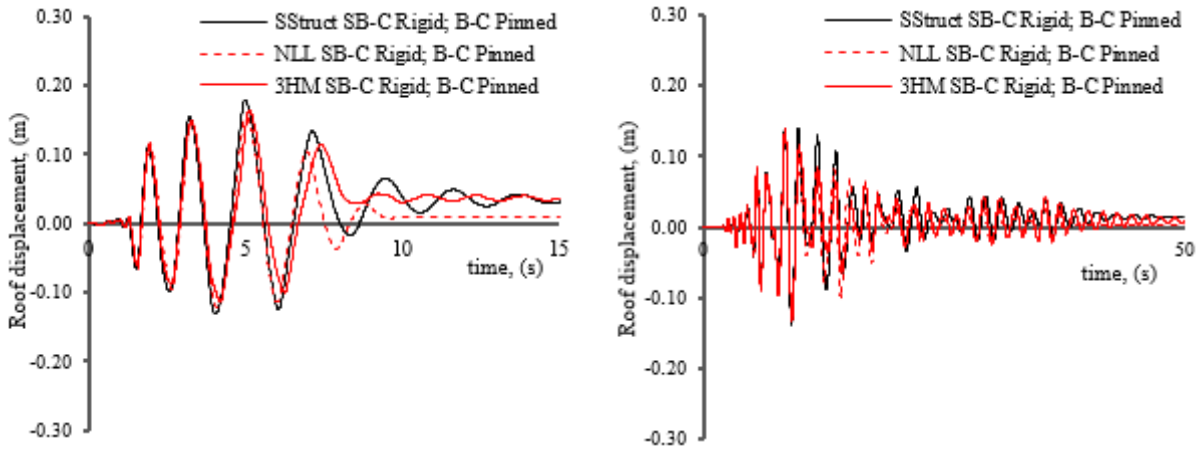

a) Hector mine accelerogram b) Kobe accelerogram

Figure 7: Comparison of 3 story CBF-MB roof displacement

It can be noticed that the maximum value of the base shear force and the roof displacement is similar for both proposed modelling techniques. A good agreement between the time histories of roof displacements and base shear for the examined FE models can be noticed. This is indicative of the adequacy of the proposed modelling techniques. A more pronounced difference may be noted in the magnitude of residual displacements. The NLL model exhibits lower residual displacement values than those of the 3HM and SeismoStruct fibre models. This can be explained with the characteristics of the Multi-linear Plastic Link with Pivot hysteresis type. As discussed in point 3.1, the typical pinching of a single brace hysteretic response cannot be simulated accurately in reverse tension loading, resulting in overestimated brace stiffness. This results in unrealistically low residual roof displacement values.

On the other hand, 3HM can provide an accurate prediction of the brace hysteresis behaviour which reflects in more realistic residual drift results. The agreement of the residual displacements values between the 3-Hinge model and the fibre FE SeismoStruct model indicates that 3HM can simulate reliably the self-centering capability of the CBF-MB.

It should be noted that all three models produce similar results. The NNL model cannot capture precisely the residual drifts of the CBF-MB but the analyses of the NNL model require significantly reduced computation time and convergence is reached with fewer zero steps.

4 CASE STUDY - 2D FRAME

4.1 Geometry and general assumptions

The case study presented below is based on a 2-D CBF-MB extracted from a three-storey building, Figure 8. The building frame comprises three 8m bays with nominally pinned beam-to-column joints and pinned column bases. Hot rolled HEA profiles for columns and IPE profiles for floor beams are used. No composite action with the concrete slab is considered. Each CBF-MB is integrated in the middle of the bay. Thus the main loads of the braced frame columns are primarily axial resulting from the seismic action, and the remaining frame columns carry the gravity loads. A similar design approach may be seen in [14], [15], [16]. The CBF-MB system was designed according to [5] by a multi-modal response spectrum analysis. The cross sections of the building frames and of the CBF-MB system are summarized in Table 2.

4.2 Materials

Steel S235 is used for the modified braces and S355 steel is adopted for CBF columns. The CBF floor beams and the splitting beams are designed with steel grade S275. The floor slab design requires C25/30 concrete and B500B reinforcing steel. The building-frame members are designed with S275 steel.

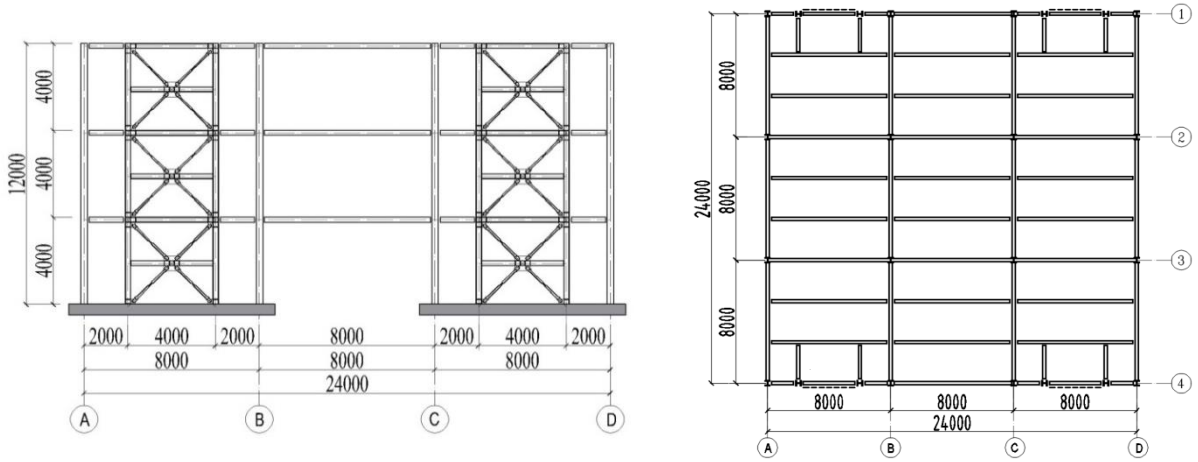

a) b)

Figure 8: 2-D building frame and building plan

Storey	CBF-MB			Building Frame			
	Braces[1]	Columns	Beams	Splitting beams	External columns	Internal columns	Beams
1	F95.6W120.5-M180.45-T16	HEA 260	HEA 240	HEA 260	HEB 500	HEB 500	IPE 360 IPE 500

[1] The MB cross sections will be described by abbreviations that should be read as follows: F (flange) 95.6 width 95 mm, thickness 6 mm; W (web) 120.5 width 120 mm, thickness 5 mm; – M (modified section) 180.45 length 180 mm, flange width 45 mm – T16 (web thickness of MS) 16 mm.

2	F85.5W120.5-M180.35-T14	HEA 260	HEA 240	HEA 240	HEB 500	HEB 500	IPE 360 IPE 500
3	F75.4W90.4-M180.35-T12	HEA 260	HEA 240	HEA 240	HEB 500	HEB 500	IPE 360 IPE 500

Table 2: Cross sections of CBF-MB and building frame

4.3 **Loads and combinations**

Table 3 summarizes the assumptions for gravity loads and seismic action parameters. The assumed top floor loads are as those for an occupied roof terrace.

Vertical loads	
Structure self-weight	3,00 kN/m^2
Other permanent loads (ceiling, raised floor)	
– Intermediate floors	0,75 kN/m^2
– Roof floor (terrace)	1,35 kN/m^2
Perimeter walls, storey height 4 meters	2,40 kN/m
Imposed loads (category B + movable partitions):	
– Intermediate floors	3,00 kN/m^2
– Roof floor (terrace)	2,00 kN/m^2
Seismic action	
Design response spectrum for elastic analysis	Type 1
Reference peak ground acceleration (PGA)	$a_{g,R} = 0{,}32g$
Importance class II	$\gamma_I = 1{,}0$
Ground type	B ($T_B = 0{,}15$ s, $T_C = 0{,}50$ s)
Proposed behaviour factor q	5,0
Damping ratio	5%
Factors for storey occupancy in seismic design situation	$\varphi = 0{,}80$
Seismic combination coefficient	$\psi_2 = 0{,}60$, $\psi_E = 0{,}48$

Table 3: Loads and actions

The seismic floor masses per braced frame are calculated according to [4] and the results are summarized in Table 4. It is assumed that the total seismic mass is distributed equally between both CBF-MB in axes 1 and 4. No torsional effects from eccentricities of story masses have been taken into consideration in this case study.

Floor 1 mass = 82,05 t	Floor 2 mass = 82,05 t	Floor 3 mass = 82,35 t

Table 4: Seismic masses per braced frame

5 STATIC NON-LINEAR ANALYSIS WITH VARIATION OF FRAME JOINTS

The effect of frame joint stiffness on the capacity curves of the three-storey CBF-MB was determined by means of a static nonlinear analysis (SNA). Three FE models with concentrated plasticity were created in SAP2000. A variation of the type of beam-to-column joints was introduced. A Flush End Plate (FEP) partial strength joint was considered as appropriate for representing a semi-rigid connection since it was considered as the most appropriate type for beam-to-column joint in case of existence of compression force (Figure 9 b). Three joint types were used in turns – a rigid, a nominally pinned and a semi-rigid joint. Their locations and

types are presented briefly in Table 5. The created models account for the non-linear behaviour of the beam, the splitting beam, the columns, and the braces, using M-N-Hinges and P-Hinges respectively. A static nonlinear analysis was performed with a lateral force pattern in an inverted triangular type (first mode). The *P*–Δ effects were accounted for by an inclined leaning column simulating the initial sway imperfection of the frame according to [4].

Model abbreviation	Splitting beam-to-column joint (SB-C)	Floor beam-to-column joint (B-C)
SB-C Rigid; B-C Pinned	rigid, full strength	nominal pinned
SB-C Rigid; B-C PR	rigid, full strength	FEP, semi-rigid, partial resistance
SB-C PR; B-C PR	semi-rigid, partial resistance	FEP, semi-rigid, partial resistance
SB-C Rigid; B-C PR2	rigid, full strength	FEP, semi-rigid, partial-strength, from both sides of the column

Table 5: Description of the beam-to-column joint types and their locations

The structural performance was assessed by introducing three limit states related to IO (immediate occupancy), LS (life safety) and CP (collapse prevention). It was done by N2-Method [17] techniques and scaling the PGA with factors 0.5, 1.0 and 1.5 respectively for IO, LS and CP. The resultant capacity curves with indicated limit states are illustrated in Figure 9 a). The plastic mechanism at ULS features considerable and regular yielding of tension braces and buckling in compressed members along the building height, and the contour frame remains elastic. The CP limit state is characterized by brace yielding and buckling and additional flexural yielding of the splitting beam.

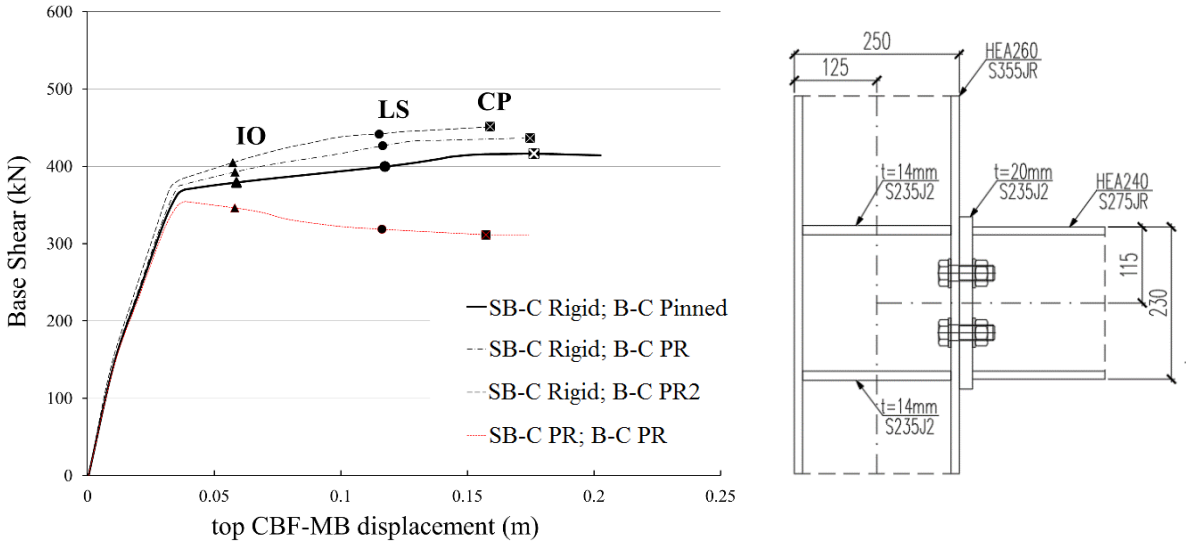

a) Capacity curves obtained through joint type variations

b) FEP beam-column joint

Figure 9: Comparison of the capacity curves of CBF-MB with variation of the joints

The capacity curves in the first three cases (SB-C Rigid; B-C Pinned, SB-C Rigid; B-C PR, SB-C Rigid; B-C PR2) are quite similar in shape. It can be noticed that using FEP for floor beam-to-column joints increases the overstrength of the system and introduces a slight reduc-

tion in ductility. The SB-C PR; B-C PR model demonstrates the role of the joint between the splitting beam and the contour frame. Neglecting the constitution of rigid joints between splitting beam and columns produces a loss of overstrength, reduction of ductility and a resultant softening inelastic branch due to domination of second order effects. In conclusion, the type of floor beam-to-column connections does not affect the system behaviour in a major way and, therefore, such connections may be designed as nominally pinned or semi-rigid. It is recommended that splitting beams are rigidly connected to the columns and thus forming internal H-frame that provides backup of lateral stiffness for the system in the range of inelastic brace behaviour and a self-centering capacity as well.

6 INCREMENTAL DYNAMIC ANALYSIS

The CBF-MB system was studied using the Incremental Dynamic Analysis (IDA) presented by Vamvatsikos and Cornell [18], [19] and FEMA-P695 [20]. The procedure adopted below is based on the relation between the Intensity Measure (IM) and the Damage Measure (DM). IM in the examined system is represented by the matched signal spectral acceleration corresponding to the structural first natural mode of vibration considering a 5% viscous damping $S_a(T_1,5\%)$, and the DM is defined using the maximum interstorey drift of θ_{max} or residual drifts, respectively. In order to generate the IDA curves, the ground motions were scaled by factors 0.50; 0.75; 1.00; 1.25; 1.50 and higher until a numerical non-convergence was reached.

Based on the conclusions made from SNA, only three of the four FE models examined in point 5 have been analyzed here using the IDA procedure - SB-C Rigid; B-C Pinned, SB-C Rigid; B-C PR, SB-C PR; B-C PR.

6.1 Ground motion records

A family of ground motion records obtained from Far-Field-Record set with PGA not much larger than 0.32g was selected. The set includes ten real records of the strongest horizontal ground motions from the PEER NGA database, with magnitudes of 6.5 or more, and refers to sites located 10 or more kilometres from a fault rupture. Adjusting of the selected strong ground motion records was achieved through the software SeismoMatch [21]. Matching of the records was based on [4] rules for recorded accelerograms. The adjusting process was performed for all ten signals. Initially, scale factors of 1.3, 1.5 and 1.5 were applied to records No 2, 3 and 5 respectively, and the remaining records were processed without scaling. The list of selected strong ground motion records and their basic characteristics is shown in Table 6 and the corresponding response spectrums are illustrated in Figure 10. The Eurocode type 1 Response Spectrum (RS), based on PGA 0,32g and Soil Type B was used. The Mean Matched RS of the matched accelerograms, the TRS and the 90% TRS are shown in Figure 11. The mean spectral response, calculated from all of the 10 records in the range of periods between 0.18 s and 2.0 s, deviates less than 2% from the corresponding TRS values. The maximum misfit is 5.1%. The processing of the records complies fully with the EN 1998-1 prescriptions and is considered suitable for evaluating the performance of the CBF-MB system related to influence of joint types.

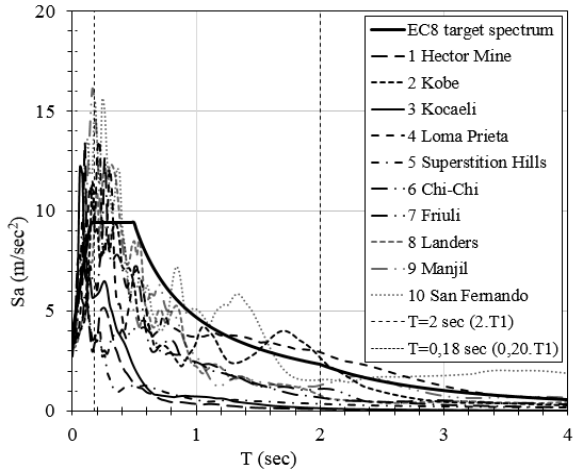

Figure 10: Response spectrums of the recorded accelerograms and Target Response Spectrum

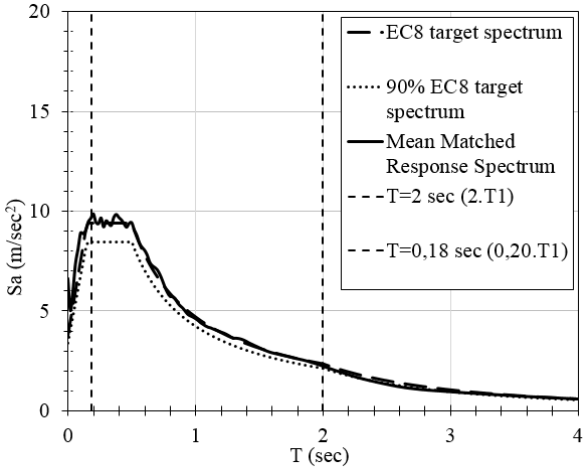

Figure 11: Target Response Spectrum, 90% Target RS and Mean Matched RS

Earthquake				Recording Station	Recorded Motions		Matched Motions	
ID №	M	Year	Name	Name	PGA max (g)	PGV max (cm/s)	PGA max (g)	PGV max (cm/s)
1	7.1	1999	Hector Mine, USA	Hector (90)	0.34	42	0.52	32
2	6.9	1995	Kobe, Japan	Kakogawa (CUE90)	0.34	23	0.33	31
3	7.5	1999	Kocaeli, Turkey	Duzce (270)	0.35	11	0.67	31
4	6.9	1989	Loma Prieta, USA	090 CDMG	0.39	45	0.34	45
5	6.5	1987	Superst. Hills, USA	Poe Road (temp)	0.35	10	0.52	40
6	7.6	1999	Chi-Chi, Taiwan	TCU 045	0.36	22	0.52	49
7	6.5	1976	Friuli, Italy	Tolmezzo (000)	0.35	22	0.52	69
8	7.3	1992	Landers, USA	Coolwater	0.33	30	0.34	32
9	7.4	1990	Manjil, Iran	Abbar	0.51	54	0.44	40
10	6.6	1971	San Fernando, USA	LA-Hollywood Stor	0.21	19	0.49	38

Table 6: List of selected strong ground motion records

6.2 **Estimation of the maximum interstorey drift**

The incremental curves of the maximum interstorey drift ratio related to signal spectral acceleration $Sa(T_1;5\%)$ are presented in Figure 12. The results for each of the models are summarized in their 16%, 50% and 84% percentiles (Figure 13).

It can be seen from Figure 12 and Figure 13 that the maximum interstorey drift ratios do not differ significantly for the three FE models. In the range of interstorey drifts larger than the prescribed by FEMA-356 [22] LS=1.5%, model SB-C Rigid; B-C Pinned indicates slightly higher interstorey drifts at the same IM level compared to the other two models. The interstorey drift ratios of the other two models (SB-C PR; B-C PR and SB-C Rigid; B-C PR) are similar. It can be concluded that the joint types do not have any major effect on the maximum interstorey drift ratios of the studied CBF-MB system.

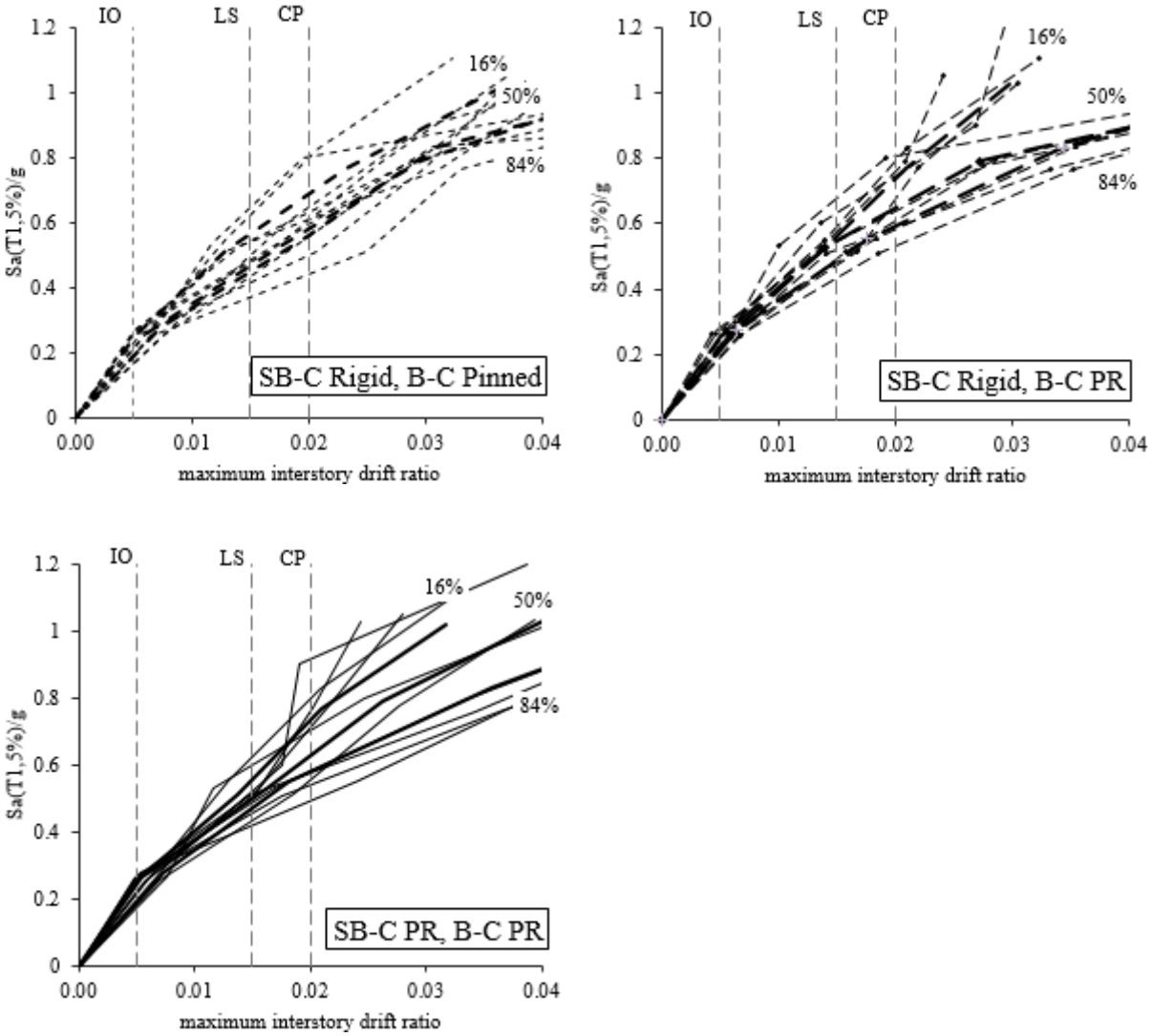

Figure 12: IDA study for 10 records on a T_1=0.881 s, 3-story CBF-MB with percentile curves of the maximum interstorey drift

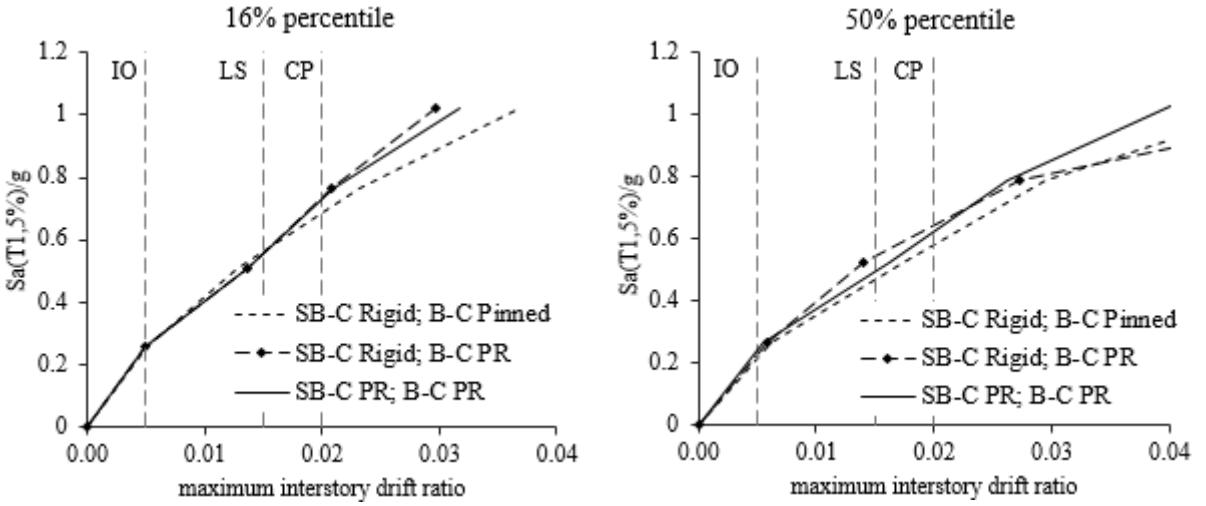

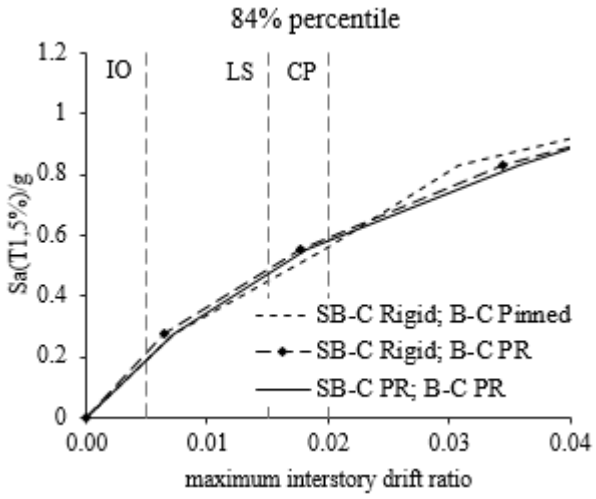

Figure 13: IDA 16%, 50% and 84% percentile of the maximum interstorey drift

6.3 **Estimation of residual interstorey drift**

The performance of the three FE models used in the study was also estimated through the incremental curves of the residual drift ratios at several IM levels (Figure 14).

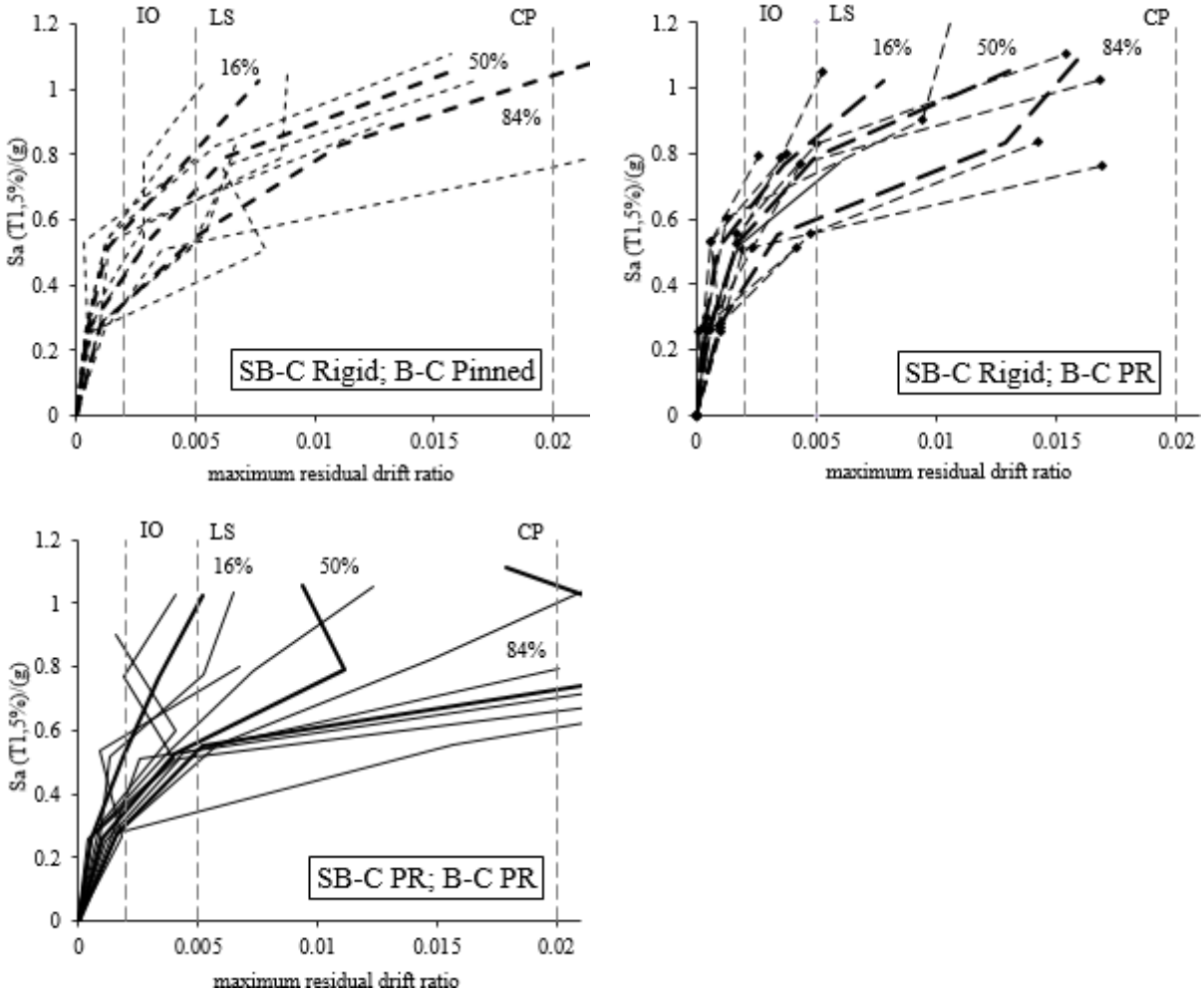

Figure 14: IDA study for 10 records on a T1=0.881 s, 3-story CBF-MB with percentile curves of the maximum residual drift ratio

The results for each model are summarized in their 16, 50 and 84 (Figure 15) percentiles and some conclusions have been drawn. The residual storey displacements are assumed to be the maximum value of the final one hundred steps in the analysis. There is a minor scatter of the results in the final steps but as this approach is practical, it produces conservative values and simplified damping effects at the end of the analysis. It should be mentioned that each signal has been elongated by approximately 25% of the original time with no accelerations, allowing capture of the residual displacement.

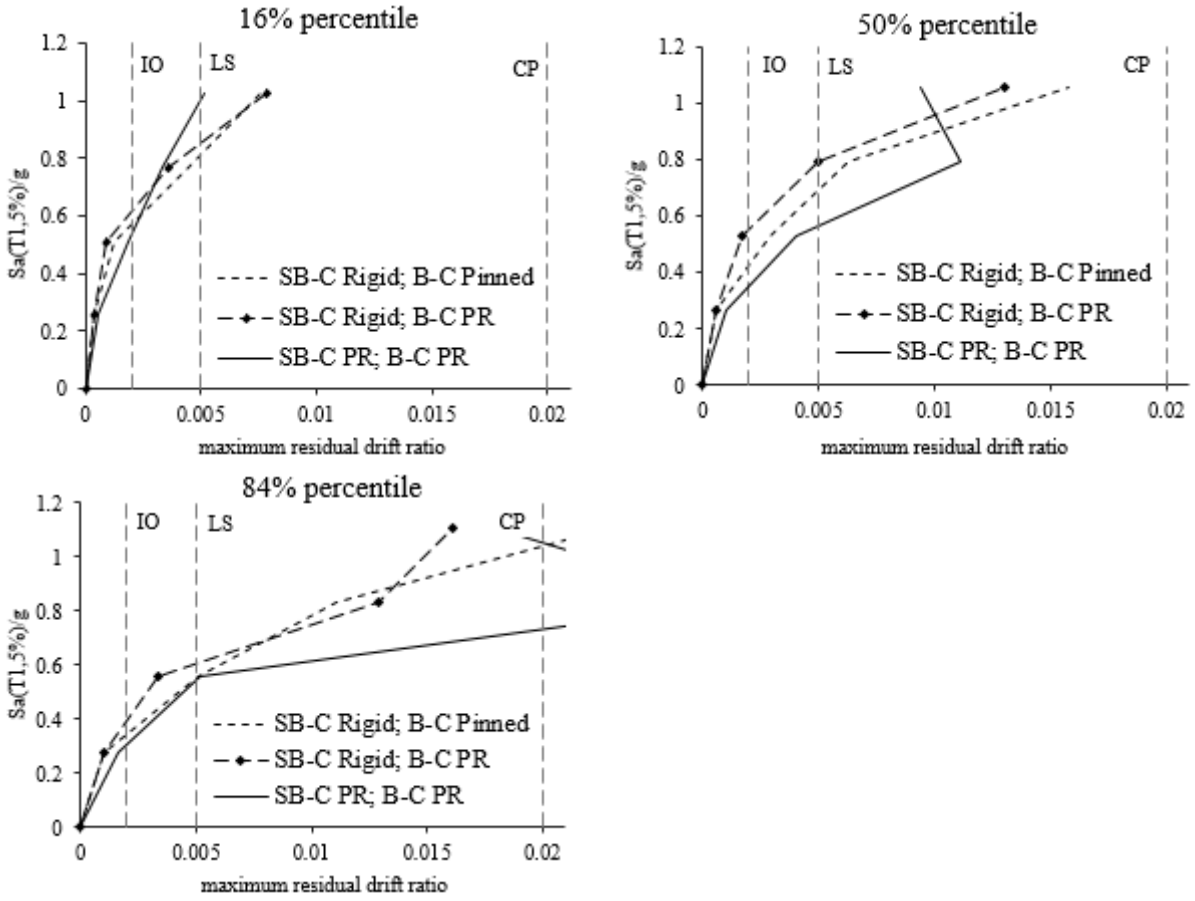

Figure 15: IDA 16%, 50% and 84% percentile of the maximum residual drift

The comparison of the 16%, 50% and 84% percentiles indicates that the SB-C PR; BC-PR model develops the highest residual drift ratios and that the SB-C Rigid; BC-PR model develops the lowest residual drift ratios. The incremental curves presented in Figure 15 are indicative of the influence of the splitting beam-to-columns joint stiffness on the self-centering capability of the CBF-MB system. It can be concluded that using rigid joints between splitting beams and columns lowers the residual displacement values and provides a self-centering capacity of the system.

Table 7 summarizes the residual maximum interstory drifts and their 16, 50 and 84 percentiles at the corresponding limit states defined by FEMA-356, namely IO (immediate occupancy), LS (life safety) and CP (collapse prevention). The values of the maximum residual drifts, reported in Table 9, were obtained by scaling the already matched signals from Table 6 by factors of 0.5, 1.0 and 1.5 respectively for IO, LS and CP and by choosing the highest storey residual drift of the ten signals.

Ground motion	Model	IO	LS	CP
Hector Mine, USA	SB-C Rigid; B-C Pinned	0.05	0.48	0.65
	SB-C Rigid; B-C PR	0.04	0.24	0.43
	SB-C PR; B-C PR	0.03	0.39	0.19
Kobe, Japan	SB-C Rigid; B-C Pinned	0.04	0.13	0.86
	SB-C Rigid; B-C PR	0.07	0.17	0.35
	SB-C PR; B-C PR	0.06	0.36	0.73
Kocaeli, Turkey	SB-C Rigid; B-C Pinned	0.04	0.28	0.28
	SB-C Rigid; B-C PR	0.04	0.18	0.60
	SB-C PR; B-C PR	0.09	0.13	0.53
Loma Prieta, USA	SB-C Rigid; B-C Pinned	0.10	0.54	0.67
	SB-C Rigid; B-C PR	0.10	0.47	1.42
	SB-C PR; B-C PR	0.16	1.57	3.80
Superstition Hills, USA	SB-C Rigid; B-C Pinned	0.12	0.36	2.03
	SB-C Rigid; B-C PR	0.10	0.20	1.69
	SB-C PR; B-C PR	0.13	0.26	2.55
Chi-Chi, Taiwan	SB-C Rigid; B-C Pinned	0.10	0.14	0.58
	SB-C Rigid; B-C PR	0.09	0.17	0.50
	SB-C PR; B-C PR	0.16	0.58	1.48
Landers, USA	SB-C Rigid; B-C Pinned	0.06	0.30	1.30
	SB-C Rigid; B-C PR	0.04	0.13	0.94
	SB-C PR; B-C PR	0.09	0.40	0.15
Manjil, Iran	SB-C Rigid; B-C Pinned	0.04	0.13	0.39
	SB-C Rigid; B-C PR	0.11	0.06	0.38
	SB-C PR; B-C PR	0.18	0.09	0.67
San Fernando, USA	SB-C Rigid; B-C Pinned	0.07	0.79	0.61
	SB-C Rigid; B-C PR	0.02	0.42	0.00
	SB-C PR; B-C PR	0.11	0.43	3.09
Percentile 16%	SB-C Rigid; B-C Pinned	0.04	0.13	0.45
	SB-C Rigid; B-C PR	0.04	0.09	0.36
	SB-C PR; B-C PR	0.05	0.19	0.34
Percentile 50%	SB-C Rigid; B-C Pinned	0.06	0.29	0.63
	SB-C Rigid; B-C PR	0.06	0.17	0.50
	SB-C PR; B-C PR	0.10	0.40	1.11
Percentile 84%	SB-C Rigid; B-C Pinned	0.10	0.51	1.11
	SB-C Rigid; B-C PR	0.10	0.34	1.29
	SB-C PR; B-C PR	0.16	0.52	2.85

Table 7: Residual maximum drift ratio in %

The criteria for the admissible residual drifts corresponding to the structural performance levels of CP, LS and IO are presented in Table C1-3 of FEMA-356 [22]. The residual drift ratios should, according to the table, be lower than or equal to 2% for CP, lower than or equal to 0.5% for LS, and negligible for IO. The authors have adopted these criteria and propose a residual drift ratio of 0.2% as the criterion for IO, this value being consistent with the essen-

tial tolerance for multi-storey frames according to EN 1090-2 Table C.2.4 [23] It should be noted that Eurocode 8 [4] does not specify any residual drift criteria.

The study shows that the residual drift criteria for LS have been exceeded for the Loma (1.57%) and ChiChi (0.58) signals in the SB-C PR; B-C PR model. The same is true of the Loma (0.54%) and San Fernando (0.79%) signals in the SB-C Rigid; B-C Pinned model.

The CP residual drift criteria are exceeded for the Loma (3.8%), Superstition (2.55%) and San Fernando (3.09%) signals in the SB-C PR; B-C PR model. The residual drift in the SB-C Rigid; B-C Pinned model used for the San Fernando signal is 2.03%.

These results indicate that the SB-C Rigid; B-C PR model satisfies all the residual drift requirements of FEMA-356, and that the SB-C PR; B-C PR and SB-C Rigid; B-C Pinned models exhibit higher residual drift ratios in a few cases. Ensuring the required self-centering capabilities of the CBF-MB model would need high rotational stiffness of the splitting beam-to-column and beam-to-column joints, or even designing of these joints as rigid. The joint rotational stiffness for the SB-C PR; B-C PR model was estimated as for a FEP connection, but higher stiffness as in an extended endplate is recommended.

The 0.20% criterion proposed by IO is satisfied by all models for all signals.

7 CONCLUSIONS

This report presents an investigation on the behaviour of concentrically braced frames with modified braces (CBF-MB). Two types of brace modelling techniques are proposed and have been verified through a series of nonlinear analyses. It can be concluded that both proposed methods for modelling of the modified braces simulate effectively the overall system behaviour. The 3HM model represents precisely the single modified brace hysteresis behaviour and captures precisely the residual drifts while the NNL model saves computational time but underestimates system residual drifts. The analytical investigation reveals that the CBF-MB self-centering capabilities can be successfully controlled by appropriate design of splitting beam-to-columns joints. In order to ensure sufficient self-centering capacity and low values of residual drifts joints between splitting beams and columns, the joints need to be designed as rigid or semi-rigid but with significant rotational stiffness. From this perspective, pinned joints between splitting beams and columns are not recommended in the proposed CBF-MB system and should be avoided. A need for criteria for assessment of the system residual drifts prescribed by the European standards EN 1998-1 [4] is arised.

REFERENCES

[1] Georgiev Tzv., “Study on seismic behaviour of “X” CBFs with reduced diagonal sections”, PhD Thesis (in Bulgarian), UACEG, Sofia 2013.

[2] Tzvetan Georgiev, „Improvement of X-CBF hysteresis behaviour by introduction of MCS”, 8th Hellenic National Conference on Steel Structures, Tripoli, Greece, 2-4 October 2014, page 75.

[3] Georgiev Tzv., L. Raycheva, „Influence of splitting beam and column stiffness on CBFs ductile behaviour“, EUROSTEEL 2017, September 13–15, 2017, Copenhagen, Denmark (Articles in Press).

[4] Eurocode 8: Design of structures for earthquake resistance - Part 1: General rules, seismic actions and rules for buildings; EN 1998-1:2004.

[5] Georgiev Tzv., Zhelev D., Raycheva L., Rangelov N.," INNOSEIS - Valorization of innovative anti-seismic devices", work package 6 – deliverable 6.2 specifications for device manual, European Commission Research Programme of the Research Fund for Coal and Steel, (Article in Press).

[6] R. K. Dowell, F. Seible and E. L. Wilson, "Pivot Hysteresis Model for Reinforced Concrete Members," *ACI Structural Journal*, pp. 607-617, 1998.

[7] SAP2000, CSI, Computers and Structures Inc., www.csiberkeley.com.

[8] J. Chaboche, "A review of some plasticity and viscoplasticity constitutive theories," *International Journal of Plasticity*, vol. 24, no. 10, pp. 1642-1693, 2008.

[9] ANSYS Release 14.0 Documentation, Theory reference for ANSYS and ANSYS workbench 14.

[10] ECCS, "Study of Design of Steel Buildings in Earthquake Zones", Technical Committee 1 – Structural Safety and Loadings; Technical Working Group 1.3 – Seismic Design. 1986.

[11] Metallic materials – Tensile testing – Part 1: Method of test at room temperature; ISO 6892-1:2009

[12] Seismosoft [2014] "SeismoStruct v7.0 – A computer program for static and dynamic nonlinear analysis of framed structures," available from http://www.seismosoft.com.

[13] M. D'Aniello, G. La Manna Ambrosino, F. Portioli and R. Landolfo, "Modelling aspects of the seismic response of steel concentric braced frames", *Steel and Composite Structures*, Vol. 15, No. 5, pp. 539-566, 2013.

[14] Georgia Dougka, Danai Dimakogiannia and Ioannis Vayas, "Seismic behavior of frames with innovative energy dissipation systems (FUSEIS 1-1)", *Earthquakes and Structures*, Vol. 6, No. 5 (2014) pp. 561-580.

[15] Georgia Dougka, Danai Dimakogianni, Ioannis Vayas, "Innovative energy dissipation systems (FUSEIS 1-1) — Experimental analysis", *Journal of Constructional Steel Research Vol. 96*, May 2014, pp 69–80.

[16] Vayas, I., Dougka, G., Dimakogianni, Umbau und Erweiterung des Kindergartens der Deutschen Schule Athen. Bauingenieur 2014; 6:253-260.

[17] Fajfar P., Gaspersic P., "The N2 Method for the Seismic Damage Analysis of RC Buildings", *Earthquake Engineering and Structural Dynamics*, Vol. 25, 31-46, 1996.

[18] Vamvatsikos D., Cornell C.A. The incremental dynamic analysis and its application to performance-based earthquake engineering. In: *Proc.12th European Conference on Earthquake Engineering*; 2002; 479; London.

[19] Vamvatsikos D, Cornell CA. Incremental dynamic analysis. *Earthquake Engineering and Structural Dynamics 2002*; Vol. 31, Issue 3, pp. 491-514.

[20] FEMA – P695: Quantification of building seismic performance factors, Washington; 2009.

[21] Seismomatch v.2.1.0, Seismosoft, http://www.seismosoft.com.

[22] FEMA – 356: Prestandard and Commentary for the seismic rehabilitation of Buildings. Washington; 2000.

[23] Execution of steel structures and aluminium structures – Part 2: Technical requirements for steel structures; EN 1090-2:2008